Med Chem Res (2015) 24:3483–3493
DOI 10.1007/s00044-015-1405-x

MEDICINAL CHEMISTRY RESEARCH

ORIGINAL RESEARCH

Differential algorithms-assisted molecular modeling-based identification of mechanistic binding of ganoderic acids

Balraj Singh Gill[1] · **Sanjeev Kumar**[1]

Received: 14 October 2014 / Accepted: 28 June 2015 / Published online: 9 July 2015

Abstract *Ganoderma*, in the recent years, has been comprehensively characterized and held invaluable for their miscellaneous pharmacological activities. Recently, attempts to explore and fathom the pathway of inhibition revealed GA-A and GA-H to impede the progression of breast cancer by inhibiting the signaling of AP-1 and NF-κB, although the mechanism has not yet been explored. NF-κB is a key transcription factor having irrefutable role in cell proliferation, apoptosis and cancer signaling and its subunits κB-IKKα, IKKβ and IKKγ (NEMO) are pivotal to the cancer signaling mechanism. The present study confirmed mechanistically the association between NF-κB and NEMO in regulating the signaling cascade of NF-κB. GA-A and GA-H were observed to participate in various non-covalent interactions, thus contributing largely to the stability of the ligand–macromolecules association as well as their role as anticancer agent in breast cancer. Amino acids, Lys90 and Asn732, were seen to be critically involved in the signaling cascade. Apart from this, residues Glu98 and Met94, Cys95 and Glu91 were involved in hydrogen bonding in GA-A and GA-H. The anticancer activity exhibited by GA-A and GA-H is attributed to certain docking poses and interaction that were found to be absent in the GA-F such as hydroxylation at 3 and 7 and/or 15 in the lanostane structure. This study is the first of its kind elucidating a possible mode of binding of ganoderic acid in NF-κB signaling pathway using molecular modeling studies, further evaluated by differential calculation-based algorithms.

Keywords Ganoderic acids · NEMO-IKK domain · Molecular studies

Introduction

Nuclear factor kappa B (NF-κB), a ubiquitous transcription factor, is implicated in various pivotal cell signaling responses involved in the immune response, differentiation, cell proliferation and apoptosis. Under normal conditions, NF-κB complex is sequestered with inhibitor protein IBs, in the cytoplasm. In the presence of any stimuli, the NF-κB complex undergoes phosphorylation and simultaneous ubiquitination of IBs, causing degradation and subsequent translocation of NF-κB complex from cytoplasm to the nucleus (Fig. 1). Deviations from normal signaling cascade of NF-κB pathway result in various abnormalities such as rheumatoid arthritis, asthma, inflammatory bowel disease (Tak and Firestein 2001), AIDS and cancer (Dolcet *et al.*, 2005; Giuliani *et al.*, 2001). Recent reports indicate the synchronized phosphorylation of specific amino acid residues to trigger the inception of cascade of events that accelerate the activation and subsequent translocation of NF-κB. IKK complex is an essential key regulatory element possessing two kinase subunits—IKKα (IKK1) and IKKβ (IKK2) along with a third regulatory subunit IKKγ, commonly known as NEMO (NF-κB essential modulator). IKK-β is vital for phosphorylation of IκBα on Ser 32 and Ser 36 and of IκBβ on Ser 19 and Ser 23, thus inhibiting the sequestration of NEMO/IKKβ complex assembly by imposing different inhibitor molecules which would inhibit the NF-*K*B activation.

✉ Sanjeev Kumar
sanjeevpuchd@gmail.com;
sanjeevcbs@cup.ac.in

[1] Centre for Biosciences, School of Basic and Applied Sciences, Central University of Punjab, Bathinda 151001, India

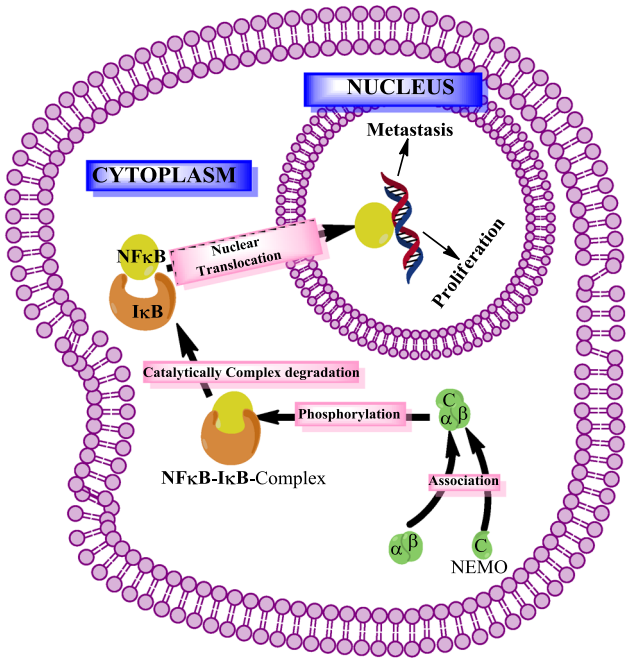

Fig. 1 Association of IKKα and IKKβ with NEMO (IKKγ) consolidates the catalytic activity of IKK complex. The IKKα and IKKβ subunit facilitates the phosphorylated catalytic cleavage of NF-κB-IkB inhibitor protein complex resulted in the free form of NF-κB, which facilitates its translocation into nucleus and turned on the mitogenic functions, cellular differentiation, proliferation, etc.

Ganoderic acids (GA) are the triterpenoids isolated from *Ganoderma* species possessing multifarious pharmacological effects. But lately, a paradigm shift has been observed in their therapeutic activities toward cancer (Suarez-Arroyo *et al.*, 2013), as Silva *et al.* and Funian *et al.* have demonstrated that their anti-cancerous role is exhibited through modulation of the signaling cascade of AP-1 and NF-κB inhibition. AP-1 and NF-κB are the two transcription factors among many others that have been proved to play an important role in the regulation of expression of urokinase-type plasminogen activator (uPA) and urokinase-type plasminogen activator receptor (uPAR). In addition, they have also found to participate in the modulation of expression of other genes involved in the cell cycle progression, cell survival, inflammatory tumor growth, etc. (Allgayer, 2010; Sliva, 2004). Literature reports have highlighted the role of constitutive activation of AP-1 and NF-κB in highly invasive breast cancer cell lines (Daschner *et al.*, 1999). In this direction, *Ganoderma* constituents, especially ganoderic acids A and H, have been observed to potently inhibit the constitutive activation, although their mechanism has not yet been clearly understood. The study performed by Jiang (Jiang *et al.*, 2008) and his research group revealed that GA-A and GA-H may be acting by inhibiting cellular proliferation, agglomeration, adherence, migration and invasion by affecting the downstream signaling of transcription factors, AP-1 and NF-κB, which as a consequence results in downregulation of Cdk4 and uPA secretion (Chen *et al.*, 2010; Jiang *et al.*, 2008). On the contrary, GA-F did not manifest these effects. The activities exhibited by ganoderic acids A and H can be attributed to the hydroxylation at 3 and 7/15 position of the lanostane ring. This research work is being put forward with an impetus to prove through docking studies that the hydroxyl group of GA-A and GA-H participates in several interactions with IKKα and IKKβ—subunits of NF-κB—that are not observed in GA-F due to the absence of the hydroxyl group. In addition, we have also sought to report several other interactions occurring between the amino acid residues and the constituent.

Structural aspects of NEMO/IKKβ-associated domain

Detailed crystal structure of the NEMO/IKKβ is retrieved from Protein Data Bank [PDB: 3BRT](Rushe *et al.*, 2008). Protein complex comprises of 4-helix chain of NEMO and IKKβ domains shown in (Fig. 2). The IKK peptide density extends from residues 705–743 in chain A and from residues 701–744 in chain C, whereas, the NEMO density extends from residues 49–109 in chain B and from 49 to 109 in chain D. The IKKα and IKKβ kinases contain kinase domain and leucine zipper where the catalytic unit dimerizes and forms a loop helix in *C*-terminal which then interacts with NEMO. Structurally, NEMO consists of two coiled region (CC1 and CC2), leucine zipper (LZ) and zinc finger (ZF) in the C-terminal. CC1 region interacts with IKK kinase *C*-terminal (Ghosh and Karin, 2002), whereas, CC2 and LZ region of NEMO are sites for trimerization or tetramerization (Agou *et al.*, 2002). IKK-binding region of NEMO was found to be in residues 47–120 in the C-terminal of IKKβ (Marienfeld *et al.*, 2006), and conserved

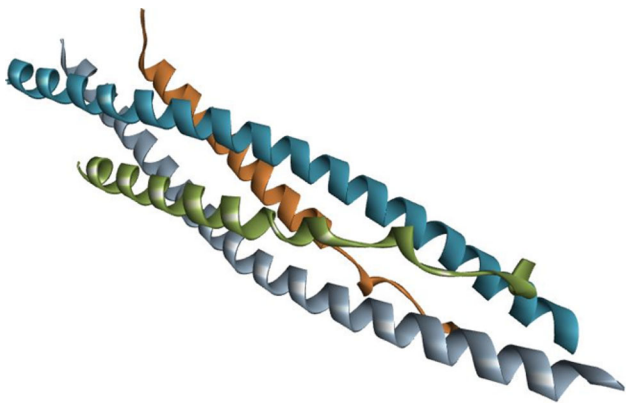

Fig. 2 Structure of NEMO/IKK-associated domains in various colors (PDB id-3BRT)

sequence known as NEMO-binding domain (NBD) L-^{737}DWSWL^{742} present in both IKKα and IKKβ (May *et al.*, 2002) plays pivotal role in complex formation inhibiting the activation of NF-κB in cancer cell line (Biswas *et al.*, 2004). Alanine scanning mutagenesis and FRET studies revealed that the D738, W739 and W741 residues were indisputably significant in NBD (May *et al.*, 2002). Further, it was observed that phosphorylation on residue S740 decreased the association in NEMO (Schomer-Miller *et al.*, 2006). Two IKK peptides are helical in structure except at the region lying between 732 and 742 owing to the interaction between the side chain of tryptophan and main chain of amides, which causes the constriction in the backbone. These unique non-helical structures of IKK peptide differentiate the NEMO-IKK-associated domain (Fasshauer *et al.*, 1998). Each IKK peptide associates with NEMO molecule loosely in the N-terminal, but tightly at two NEMO molecules at C-terminal. Cavities form specific pocket by dimeric NEMO with residue 85–101 with IKK peptide linker and NBD (Grover *et al.*, 2010).

Stability of NEMO

Hydrophobic interactions impart the much demanded stability in NEMO dimerization taking place at the N- and C-terminal. Region encompassing the *N*-terminal contains high degree of complementary spatial and electrostatic features, whereas, on the other hand, C-terminal mainly harbors hydrophobic residues. Formation of NEMO-IKKβ complex is mainly attributed to the intermolecular hydrophobic interactions occurring in between the three IKK side chains inside the NEMO pocket. The significance of the NBD residues is explained on the basis of mutation, specifically the mutation of tryptophan to phenylalanine at residue 739 or 741, which resiliently maintains the structure integrity; on the contrary, mutation of tryptophan to tyrosine does not disrupt the integrity at 739 but alters that at 741. Y739 forms intramolecular hydrogen bonding with 734 to a stable and native backbone of IKK conformation, whereas, Y741 does not show this hydrogen bonding, thus making it less stable for NEMO binding. L737 or L742 plays crucial role in NBD, but mutations in these units have also been observed to result in reduction of binding (Grover *et al.*, 2010).

Selective pockets and hot spots

Residues in the linker and NBD region participate in a critical interaction, in which mutation in the two tryptophan residues in the NBD region results in more than twofold reduction in binding energy (May *et al.*, 2002). This, as a consequence, provided the necessary impetus to design a pharmacophore bearing three hydrophobic residues, W741, W739 and M/F 738, interacting with Glu89. These three residues, which on substitution with alanine reduce the binding to 100-folds, represent the hot spots. Any factor, which causes disruption in these hot spots leads to the rupturing the structure (May *et al.*, 2002). Although many studies have presented reports on effect of ganoderic acid on suppression of NF-κB activation, these reports failed to outline the mechanism behind it. This study is a concerted effort to put forth the plausible mode of action of ganoderic acid especially the isoforms A and H on the NF-κB signaling pathway.

Methodology

The protein crystallized structure was retrieved from PDB site (PDB id: 3BRT, NEMO-IKK-associated interactive domain) from which water molecules were removed in concern to the domain topology which usually interacts with hydrophobic regions. Thereafter, polar hydrogens, wherever required, were incorporated to complete inappropriate valency of the protein atoms, resulting in increased polarizability of bonds. The increased polarizability emphasized better modeling of the structure, for the computational work being carried out, which eventually enhanced the probability of ligand–protein interactions. This processed protein structure was further evaluated for the stereochemical quality by analyzing residue-by-residue geometry as well as overall structural geometry. Most of residues were observed to be in the regions which are most favored and additionally allowed region, i.e., 97.4 and 2.6 % residues, respectively, whereas no residues were found to be present in the disallowed region (Fig. 3). These evaluations help in assessing the protein stereochemistry and, as a consequence, construct a resilient model which could form the basis of further molecular modeling studies. The next crucial step was the preparation of ganoderic acid structure, achieved on the software ChemBioDraw Office (licensed @ cambridge's soft), and subsequent energy minimizations were done by integrated force field by Accelrys Discovery Studio. Moreover, the proteins of interest as well as the ganoderic structures were saved in pdbqt format to ensure the software compatibility in Autodock 1.5.6.

Grid design

AutoGrid precalculated grid maps of interaction energies for various atom types, such as aliphatic carbons, aromatic carbons, hydrogen-bonding oxygen, with a macromolecule such as a protein, DNA or RNA prior to docking. These grid maps were then used by Autodock docking calculations to determine the total interaction energy for a ligand

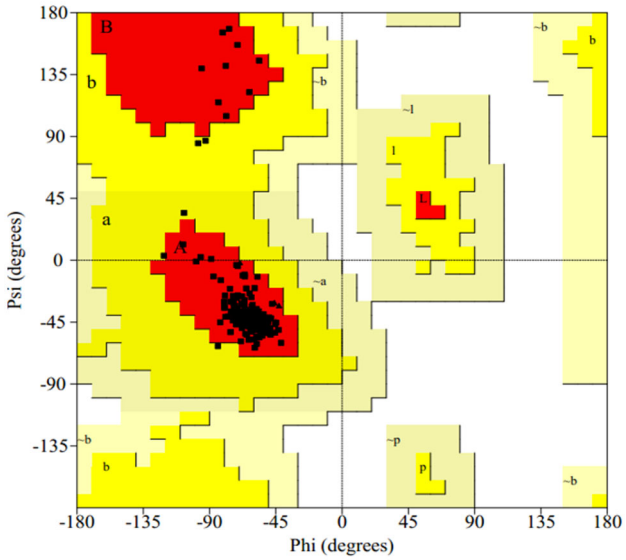

Fig. 3 Ramachandran plot of the retrieved NEMO-IKK-associated binding domain

with a macromolecule. Consequently, grid was prepared using Cygwin (@linux environment-based Windows software) as the interface to write the commands. Grid mapping, which calculated the crucial coordinates over the protein atomic data, assigned the coordinates of the NEMO-IKK-associated domain for docking. Moreover, grid mapping affords an appropriate surface topology for the ligand atoms for interaction with the NEMO-IKK-associated domain. Grid mapping is a prerequisite as, in this case, it directs the ganoderic acids to look for their region of strong affinity on the NEMO-IKK-associated domain. In present study, grid chosen incorporates the residues from 85–101, whereas energy scoring grid was prepared as a 60, 60 and 60 A° (x, y and z) with 0.375 A° spacing.

The genetic algorithm

The Lamarckian genetic algorithm (LGA) chosen to search for the best conformers makes use of mathematical concepts to simulate conditions influencing biological evolution and therefore, search for conformational space by "mutating" a ligand to find the lowest energy conformation prevalent in the "environment" of a fixed protein. It also gives proper understanding of the optimum protein ligand interactions, thereby providing the structure most likely to be found in vivo. During the docking process, a maximum of 10 conformers was considered for each compound and the population size was set to 100 with the individual conformers being initialized randomly. Maximum number of generations taken were 1000. Maximum number of top individual that automatically survived was set to 1, mutation rate was maintained at 0.02, and crossover rate was taken to be 0.8.

Rigid docking on these assigned coordinates via LGA and genetic algorithm was carried out in this work. In order to rationalize and validate docking procedure performed, two different docking algorithms were implemented at multiple times to reinforce and confirm the concept of docking methodology. Post-docking studies resulted in various conformations which were clustered on the basis of various energies. Similarly, first 10 docking poses were chosen as they were observed to possess similar profile energy levels. Keen observations revealed similar interaction between both algorithms. However, on comparison, the Lamarckian algorithm was found to exhibit higher interactions than the genetic algorithm, like Lys80, Gln83, Ala84 and Trp741 shown in Lamarckian algorithm only. Lys90, Glu91, Met94, Cys95, Gln98, Arg101, Asp732 are quite frequent and often found via both algorithms.

Selection docking poses

Autodock reports the best docking solution (lowest docked free energy) for each GA run and also performs analysis during cluster. Docking interaction was selected mainly on ligand proximity and interactions of IKKα and IKKβ with hydrophobic amino acid side chains of NEMO. Modeling studies were carried out in with PyMOL and Accelrys Viewer 3.5. PyMOL was used to calculate the distances of hydrogen bonds as measured between the hydrogen and its assumed binding partner.

Confirmation of the docking result

Initially, the crystal structure of NEMO-IKK-associated domain was retrieved from RCSB-PDB I.D. 3BRT Research Collaboratory for Structural Bioinformatics, Protein Data Bank (RCSB-PDB). This domain was further improvised by removing the embedded water molecules in the crystal structure with the assistance of Accelrys Discovery Studio Visualizer 3.5. Furthermore, polar hydrogens were added in order to complete the inappropriate valency of protein atoms. These H-atoms assisted in correction of the ionization and tautomeric states of amino acid residues. Finally, Gasteiger charges were assigned which served to improve the stereochemistry of NEMO-IKK-associated-domain-related structural issues. With the assistance of the SAVES server utility tool "Procheck," which revealed φ–ψ contour mapping, various stereochemical issues were resolved.

The structures of ganoderic acid isoforms A, F and H were prepared via ChemBio3D Ultra and energy minimized by MM2 force field where 500 iteration cycles were run and the structures were saved into pdb format (Fig. 4).

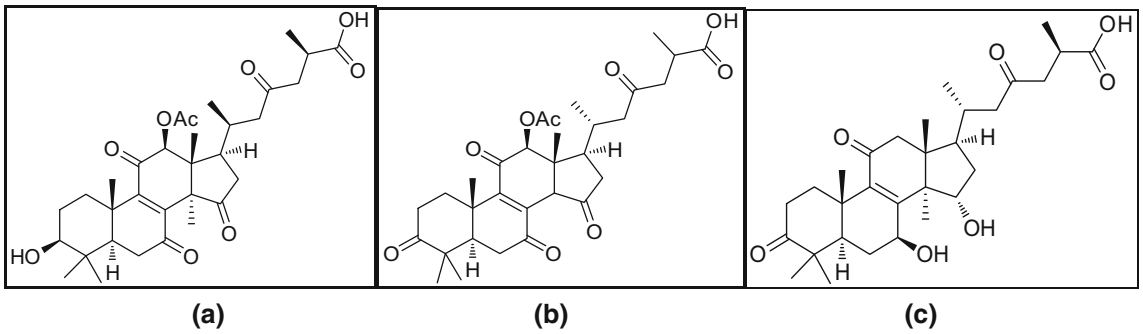

Fig. 4 Chemical structure of GA-H (**a**), GA-F (**b**) and GA-A (**c**)

These ganoderic acids possessed steroidal scaffold with only minor modification in functionalities. These modifications were inferred to play a decisive role in increasing their binding affinity and selectivity toward the NEMO-IKK-associated domain structure.

Successively, grid was generated with the aid of Auto-Grid module of Autodock. This user defined three-dimensional grid surrounding the region of interest in the NEMO-IKK-associated domain, where ganoderic acids were directed, and hence the docking site was rationalized by not docking the irrelevant areas. In the present study, the location and dimensions of the grid box was chosen such that it could incorporate the (85–101) amino acid stretch of NEMO domain involved in binding with the IKKb chains for the formation of active IKK complex. The energy scoring grid was prepared as a 60, 60 and 60 A° (*x*, *y* and *z*) cube. The spacing between grid points was 0.375 A°. The grid was formed 60 × 60 × 60 (*x*, *y*, *z*) of 15 A°. Usually larger size grid is taken to validate the proper ligand-binding site. Each docking experiment was set with 50 different runs with termination after 25,000 energy evaluation. Population size was set to be 100. LGA provided protein–ligand interaction in addition to being useful for selecting the conformation of ligand and receptor which showed the lowest energy conformation. In LGA, maximum number of energy evaluations are 1000 and the number of compounds is 50.

Results and discussion

A study performed by Jiang and his research group (Jiang *et al.*, 2008) revealed that ganoderic acids A and H portrayed potent anti-proliferative and anti-invasive activity when tested on MDA-MB-231 cell line, a highly invasive breast cancer cell line, at concentrations of 0.10, 0.25 and 0.50 mM. The results thus obtained underlined that GA-A and GA-H possessed significant potency to inhibit the growth even at low concentrations. In addition, these compounds were also observed to considerably reduce the number of colonies, inhibit cell adhesion and control the secretion of u-PA and U-PAR in the cell line under study. Taken together, this study conducted highlighted the indispensability of hydroxyl substitution on GA-A and GA-H in constitutive inhibition of NF-κB and AP-1. Keeping in view the studies performed by the research group (Jiang *et al.*, 2008), docking study was carried out between IKKα and IKKβ, subunits of NF-κB with the constituents using the Autodock software. Docking studies further confirmed the result obtained as structural activity relationship and that hydroxyl group at 3 and 7 and/or 15 in the lanostane structure of ganoderic acids A and H is crucial for biological activity and also responsible for several consequential interactions.

Docking interactions between a ligand and protein are governed by certain factors inclusive of proper orientation, conformation and position, in order to acquire possibilities of detailed molecular mechanism for calculating energy of ligands in the putative active site. Molecular binding of the isoforms of ganoderic acid with NF-κB and their confirmation as hot spots provided the much needed clue to impede the formation of NF-κB/GA complex. Impediment to the activation of the NEMO and IKKβ association by ganoderic acid constituted the mode for inactivating the complex and consequently paving the way for pharmacophore formation. Prior to docking, structure of receptor molecule was minimized using PyMOL. Binding interaction stimulated the burial or entrapment of GA within the NEMO major residues. In case of ganoderic acid, although the basic lanosterol scaffold remained the same, different substituents participated in interactions with amino acid such that they initiated events that may alter/modulate breast cancer. Homology modeling revealed the specific location on the model where the activity of ligand is highly influenced by interaction. In particular, the hydroxyl group was observed to be docked into a particular cavity, taken as a plausible mechanism for their cancer-modulating behavior. Various amino acids in exacting isoform, in this

Table 1 Comparative study of different algorithms with different parameters exhibiting best interactive residue of GA-A, GA-H and GA-F

Molecule conformation (ganoderic acid-H)	Conformation interaction with the enlisted amino acid	Binding energy	Ligand efficiency	Inhibition constant μM	Intermolecular energy	Van der Waals desolvation energy	Electrostatic energy	Total energy	Torsional energy	Unbound energy
Lamarckian genetic algorithm										
Ganoderic acid-H										
1	R87, K90, E91, C95, M94, Q98, N732	−5.29	−0.13	133.14	−7.97	−6.73	1.24	−1.41	2.68	−1.41
2	K90, E91, M94, C95, Q98, R101, N732	−4.82	−0.12	294.53	−7.5	−5.36	2.14	−1.59	2.68	−1.59
3	K90, E91, M94, C95, Q98, N732, S733, N736	−3.96	−0.1	1.25	−6.65	−5.81	0.83	−1.53	2.68	−1.53
4	Q98, R101, D738, W741	−6.24	−0.15	26.9	−8.92	−7.82	1.09	−1.3	2.68	−1.3
5	F97, Q98, R101, W741	−5.13	−0.13	173.08	−7.82	−6.06	1.76	−1.14	2.68	−1.14
6	K90, E91, M94, Q98, N732	−4.45	−0.11	544.22	−7.14	−5.59	1.55	−1.63	2.68	−1.63
7	K90, E91, M94, Q98, N732	−4.44	−0.11	556.49	−7.12	−6.1	1.02	−1.18	2.68	−1.18
8	K90, E91, M94, C95, Q98, N732	−4.57	−0.11	449.09	−7.25	−5.91	1.34	−1.5	2.68	−1.5
9	L80, Q83, A84, R87, K90, E729, N732	−4.43	−0.11	561.23	−7.12	−6.38	0.74	−0.98	2.68	−0.98
10	K90, Q98, R101, N732, D738, W741	−4.53	−0.11	481.86	−7.21	−6.08	1.13	−1.33	2.68	−1.33
Ganoderic acid-F										
1	R87, K90, E91, M94, C95, Q98, N732	−4.75	−0.12	330.01	−7.73	−6.46	1.27	−1.53	2.68	−1.53
2	K90, E91, M94, C95, Q98, R101, K102, N732	−5.45	−0.13	101.22	−8.43	−7.18	1.26	−1.06	2.68	−1.06
3	K90, C95, E91, Q98, N732, S733, N736	−4.91	−0.12	250.16	−7.9	−6.78	1.12	−0.99	2.68	−0.99
4	Q98, R101, D738, W741	−4.64	−0.11	398.84	−7.62	−5.43	2.19	−1.15	2.68	−1.15
5	F97, Q98, R101, W741	−5.08	−0.12	187.81	−8.07	−5.73	2.33	−1.35	2.68	−1.35
6	K90, E91, M94, C95, Q98, N732	−4.64	−0.11	394.61	−7.63	−5.32	2.3	−1.37	2.68	−1.37
7	R87, K90, E91, M94, C95, Q98, N732	−4.0	−0.1	1.17	−6.98	−5.74	1.24	−1.17	2.68	−1.17
8	F92, E88, C95, Q98, E99, R101, K102,	−3.87	−0.09	1.45	−6.85	−4.86	1.99	−1.37	2.68	−1.37
9	L80, E83, A84, R87, K90, N732, E729	−5.24	−0.13	145.03	−8.22	−6.5	1.72	−1.14	2.68	−1.14
10	K90, Q98, R101, N732, D738, W741	−4.65	−0.11	388.1	−7.64	−5.18	2.46	−1.32	2.68	−1.32
Ganoderic acid-A										
1	R87, K90, N732, E91, C95, M94	−4.85	−0.13	278.08	−7.83	−6.65	1.18	−0.91	2.68	−0.91
2	K90, N732, C95, E91, Q98, M94, R101, K102	−4.9	−0.13	254.23	−7.89	−6.39	1.49	−1.28	2.68	−1.28
3	K90, N732, C95, E91, M94, N736, S733	4.48	−0.12	519.73	−7.46	−5.58	1.88	−1.17	2.68	−1.17
4	Q98, R101, D738, W741	−5.05	−0.13	200.28	−8.03	−6.17	1.85	−1.05	2.68	−1.05
5	Q98, R101, F97, W741	−5.56	−0.15	84.39	−8.54	−7.03	1.51	−0.97	2.68	−0.97
6	K90, M94, C95, Q98, N732	−5.53	−0.15	88.96	−8.51	−6.19	2.32	−0.98	2.68	−0.98
7	K90, E91, M94, C95, Q98, N732	−5.57	−0.15	82.47	−8.55	−6.95	1.61	−1.0	2.68	−1.0
8	K90, E91, M94, C95, Q98, N732	−4.52	−0.12	486.72	−7.5	−5.46	2.04	−0.83	2.68	−0.83
9	L80, Q83, A84, R87, K90, E729, N732	−5.5	−0.14	92.37	−8.49	−7.24	1.25	−0.84	2.68	−0.84
10	K90, Q98, R101, N732, D738, W741	−3.86	−0.1	1.49	−6.84	−5.04	1.8	−1.29	2.68	−1.29

Table 1 continued

Molecule conformation (ganoderic acid-H)	Conformation interaction with the enlisted amino acid	Binding energy	Ligand efficiency	Inhibition constant μM	Intermolecular energy	Van der Waals desolvation energy	Electrostatic energy	Total energy	Torsional energy	Unbound energy
Genetic algorithm										
Ganoderic acid-H										
1	R87, K90, N732	−1.49	−0.04	80.34	−4.18	−3.6	0.58	−2.01	2.68	−2.01
2	K90, R87, E91, N732	−2.48	−0.06	15.19	−5.17	−4.11	1.06	−2.05	2.68	−2.05
3	R87, K90, E91, M94, C95, Q98,	−3.75	−0.09	1.79	−6.43	−5.63	0.8	−1.54	2.68	−1.54
4	R87, E91 K90, M94, C95, Q98, N732	−4.07	−0.1	1.03	−6.76	−5.97	0.79	−2.13	2.68	−2.13
5	K90, Q98, R101, N732	−1.9	−0.05	40.76	−4.58	−4.02	0.56	−1.66	2.68	−1.66
6	K90, E91, M94, Q98, N732	−4.47	−0.11	532.28	−7.15	−5.93	1.22	−1.29	2.68	−1.29
7	K90, E91, M94, C95, Q98, N732	−3.95	−0.1	1.28	−6.63	−5.21	1.42	−1.46	2.68	−1.46
8	K90, E91, M94, Q98, N732	−4.87	−0.12	268.62	−7.56	−6.31	1.25	−1.49	2.68	−1.49
9	Q98, R101	−3.5	−0.09	2.72	−6.18	−4.86	1.33	−1.22	2.68	−1.22
10	E91, C95, Q98, R101	−3.96	−0.1	1.24	−6.65	−6.17	0.48	−1.04	2.68	−1.04
Ganoderic acid-F										
1	K90, Q98, R101, N732	−3.14	−0.08	5.02	−6.12	−4.44	1.68	−0.44	2.98	−0.44
2	R87, E91, Q98, R101, K102	−3.53	−0.09	2.57	−6.52	−4.61	1.91	−1.04	2.98	−1.04
3	R87, E91, M94, C95, Q98, E99	−2.31	−0.06	20.1	−5.3	−3.42	1.88	−1.83	2.98	−1.83
4	R87, E91, M94, C95, Q98, R101, K102	−3.13	−0.08	5.04	−6.12	−3.87	2.24	−1.62	2.98	−1.62
5	Q98, R101, K102, D738, S740	−2.95	−0.07	6.85	−5.94	−3.87	2.06	−1.23	2.98	−1.23
6	E91, M94, C95, Q98, R101, K102	−3.23	−0.08	4.32	−6.21	−4.2	2.01	−1.42	2.98	−1.42
7	K90, Q98, R101, N732	−4.13	−0.1	935.23	−7.12	−5.21	1.9	−1.12	2.98	−1.12
8	K90, Q98, R101	−2.61	−0.06	12.15	−5.6	−3.64	1.96	−0.96	2.98	−0.96
9	K90, Q98, R101, N732	−2.63	−0.06	11.74	−5.62	−3.76	1.86	−1.06	2.98	−1.06
10	K90, Q98, R101, N732	−3.04	−0.07	5.95	−6.02	−4.66	1.36	−1.21	2.98	−1.21
Ganoderic acid-A										
1	R87, K90, E91, M94, C95, Q98, N732	−3.71	−0.1	1.92	−6.69	−5.57	1.12	−0.95	2.98	−0.95
2	K90, E91, M94, C95, Q98, E729, N732	−2.76	−0.07	9.45	−5.74	−4.77	0.98	−1.29	2.98	−1.29
3	R87, K90, E91, N732	−1.39	−0.04	94.95	−4.38	−3.91	0.47	−2.31	2.98	−2.31
4	K90, E91, C95, Q98, E99, R101, K102, N732	−3.67	−0.1	2.05	−6.65	−4.56	2.09	−0.81	2.98	−0.81
5	E91, C95, Q98, E99, R101, K102	−2.8	−0.07	8.88	−5.78	−3.74	2.05	−0.83	2.98	−0.83
6	K90, E91, M94, C95, Q98, N732	−3.49	−0.09	2.75	−6.48	−5.1	1.37	−0.58	2.98	−0.58
7	K90, E91, C95, N732, S733, N736	−3.33	−0.09	3.65	−6.31	−5.38	0.93	−1.23	2.98	−1.23
8	E89, K90, E91, C95, Q98, N732, S733, M734, N736	−3.2	−0.08	4.48	−6.19	−5.38	0.81	−1.1	2.98	−1.1
9	E91, M94, C95, Q98, R101, K102	−3.92	−0.1	1.35	−6.9	−5.04	1.86	−0.52	2.98	−0.52
10	R87, K90, E91, M94, C95, Q98, E729, N732	−4.91	−0.13	250.96	−7.89	−6.36	1.54	−1.22	2.98	−1.22

study, were observed to interact in disparate fashion, thus, it could be explored more proficiently for genesis of drugs. Different models were obtained from the two algorithms employed—genetic and Lamarckian algorithms—and their numerous parameters, consequential for molecular homology, were analyzed for rational docking. Among the models obtained, best ten were chosen on the basis of various constraints charted out in Table 1. Crucial interactions between the ligand and macromolecule display different binding pattern observed to be prevalent, especially in the Lys 90, Glu91 and Gln98. Moreover, these interactions are seen to be present conspicuously in all three isoform of GA, thus, showing the critical nature of interactions (Table 2). Various interactions such as hydrogen bonding, electrostatic force, van der Waals forces are commonly seen binding mechanisms in posing the lock key fitting of ligand with macromolecule and providing stability to the structure. Bond or even small hindrances to these binding molecules can cause the complex to lose the stability essential for its integrity. This provided the much sought after rationale and opportunity to design pharmacophore by congregating various steric and electronic features required for the supramolecular interaction which would eventually be able to a trigger biological response effectively. The binding behavior of GA to NEMO was significantly attributed to hydrogen bonding with Asn732 and the interaction with oxygen by capping the hydrogen bond with GA. This target was further invaded by Lys 90, thus showing its crucial site for docking. In present docked molecule, the ε-amino group (NH_3^+) of Lys90 forming the hydrogen bonding with GA-A and GA-H is considered as the decisive interaction. Lysine is known to be the major site for acetylation, ubiquitination and SUMOylation, thus a pivotal moiety to hinder complex NF-κB. This strong hydrogen bonding provides steric and thermodynamic barrier providing hindrance to the NEMO by the ligand. This leads to distortion in complex forming a thermodynamically less stable structure, which ultimately results in non-activation of NEMO/IKKb and eventually arrests its translocation to the nucleus. Significance of Lys90 in IKK complex was substantiated in patients suffering from Incontinentia pigmenti (IP).

Strong intermolecular interactions with the NEMO chains create steric barrier for the IKKβ subunit, resulting in complex formation. The binding of GA-A to NEMO is characterized prominently by hydrogen bonding to the residue Lys90 and Asn732, Glu98 and Met94, Cys95 and Glu91 which significantly modulate the signaling in cancer. Hydrogen bonding was seen to play critical role in case of residues Gln98, Arg87, Met94, Cys95 Glu91 and Lys90 found to be electron donor toward the ligand, whereas, Glu

Table 2 Frequency of the amino acid in the docking pose of GA

Amino acid	Number of frequency (GA-H)	LA-H	Amino acid	GA-F	LA-F	Amino acid	GA-A	LA-A
L80	0	1	L80	0	1	L80	0	1
A84	0	1	E83	0	1	Q83	0	1
R87	4	1	A84	0	1	A84	0	1
K90	8	8	R87	3	3	R87	3	1
E91	4	6	E88	0	1	K90	8	7
M94	5	6	K90	5	7	E91	10	5
C95	4	3	E91	4	5	M94	5	6
Q98	8	9	F92	0	1	C95	4	6
R101	3	3	M94	3	4	F97	0	1
E729	0	1	C95	3	6	Q98	8	7
N732	7	7	Q98	9	9	R101	3	4
S733	0	1	E99	1	0	K102	3	1
N736	0	1	R101	9	5	E729	2	1
D738	0	2	K102	3	2	N732	8	8
W741	0	3	N732	4	6	S733	2	1
			S733	0	1	N736	2	1
			N736	0	1	D738	0	2
			D738	0	2	W741	0	3
			W741	0	3			
			K738	1				
			S740	1				

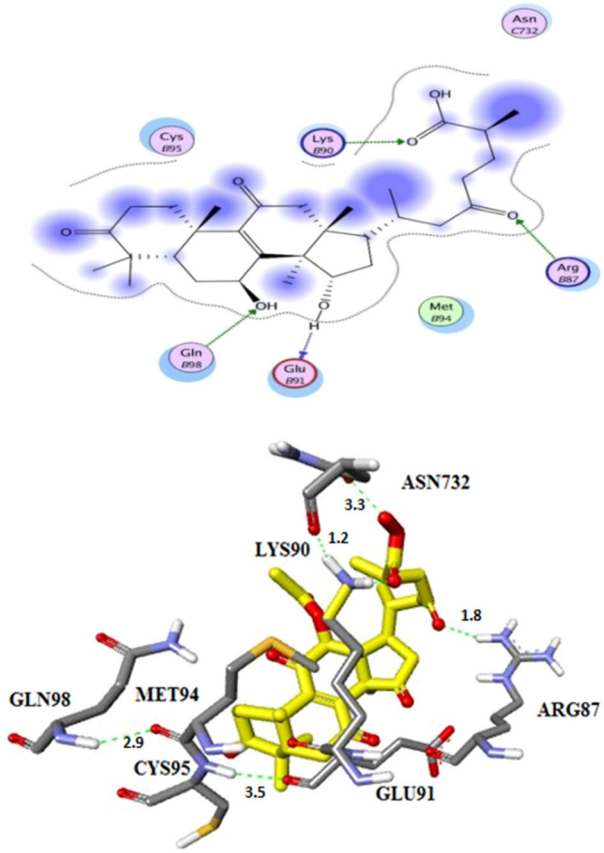

Fig. 5 Binding interaction of GA-A with NEMO showing electrostatic interaction was found in Glu77, Cys76, Asp 725 and Gln 83. Van der Waals interaction was found in Leu80, Leu718, Ala722 and Thr717. Hydrogen bonding playing critical role was seen in case of residues Gln98, Arg87, Met94, Cys95 Glu91 and Lys90 found to be electron donor toward the ligand, whereas Glu 91 was seen to be electron acceptor and formed hydrogen bonding

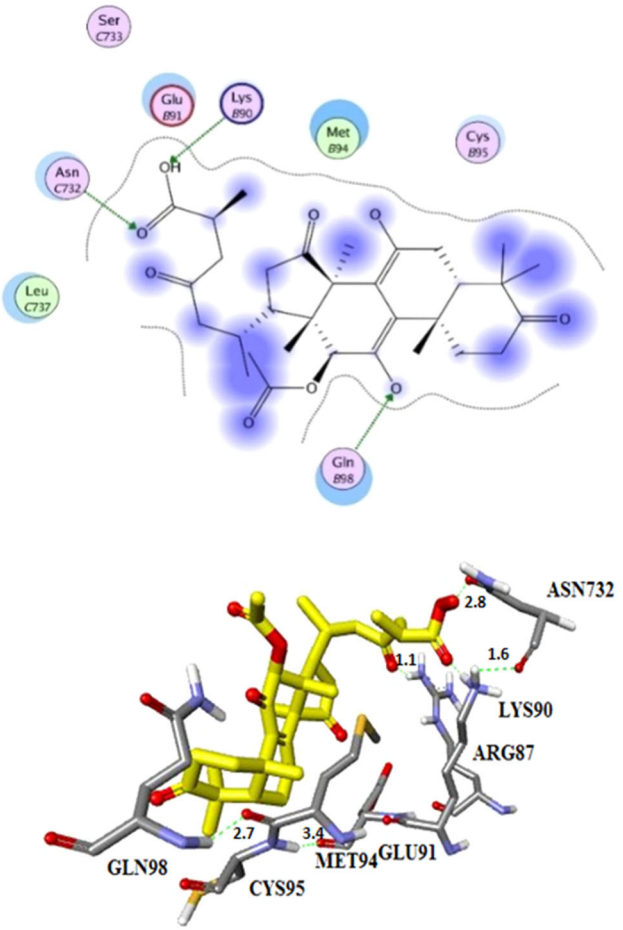

Fig. 6 In molecular docking of GA-H, binding interaction of GA-H residues with the NEMO prominently in Lys90 and Asn732, whereas hydrogen bonding was found in Lys90 and Asn732 and Glu98 and Met94, Cys95 and Glu91. Electrostatic interactions were in found in Leu737, little in Met 735 and Ser733. Van der Waals forces in Phe92, Trp739 and Ser740. These non-covalent interactions bring the stabilization in binding of ligand with macromolecules by lowering energy

91 was seen to be electron acceptor and formed hydrogen bonding. Variation in the bond distance was observed in all the lanosterol structure of ganoderic acids ranging up to 3 A°. It ranges from 1.2 A° in Asp732 and Lys90, Gln98 and Cys95 (2.9 A°), whereas Cys95 and Gln91 display 3.5 A° (Fig. 5). Electrostatic interactions were found in Leu737, little in Met 735 and Ser733, whereas, van der Waals forces were observed in residues Phe92, Trp739 and Ser740. These non-covalent interactions stabilize the binding of ligand with macromolecules by lowering energy, as shown in (Fig. 5). GA-H interactions were found in Lys90, Asn732, Glu98, Met94, Cys95, Glu91. Lys90, Asp732 and Gln98 donate electron and form hydrogen bonding with oxygen. Bond distance between Asp732 and Lys90 is 1.6 A°, Cys95 and Gln98 is 2.7 A°, whereas, between Cys95 and Met94 is 3.4 A° (Fig. 6). Lys90, Gln98 and Arg87 donate electron and form hydrogen bonding with oxygen, whereas, Glu91 accepts electron and forms bonding. Bond distance between Asp732 and Lys90 is 0.8 A°, whereas, Gln98 and Arg101 shows 2.1 and 2.4 A° distances. The residues Lys90, implicated in various anomalies, is seen to be critically involved in binding with ganoderic acid. While higher level of binding energy revealed its lower affinity for protein binding. The binding pose is disclosed in Fig. 7.

Surprisingly, ganoderic acids are frequently interacting with the residues Lys80 to Arg101 and Glu729 to Trp741. In addition, the interaction of Arg87, Lys90, Glu91, Met94, Cys95, Gln98 R101 and Asn732 with ganoderic acid suggests the plausible mechanism for accommodation of basic scaffold suitability in the cavity, irrespective of the specific functionality group, carried by the corresponding ganoderic acids. This preliminary study seeks to assiduously explore the probable active site of ganoderic acid on the NF-κB.

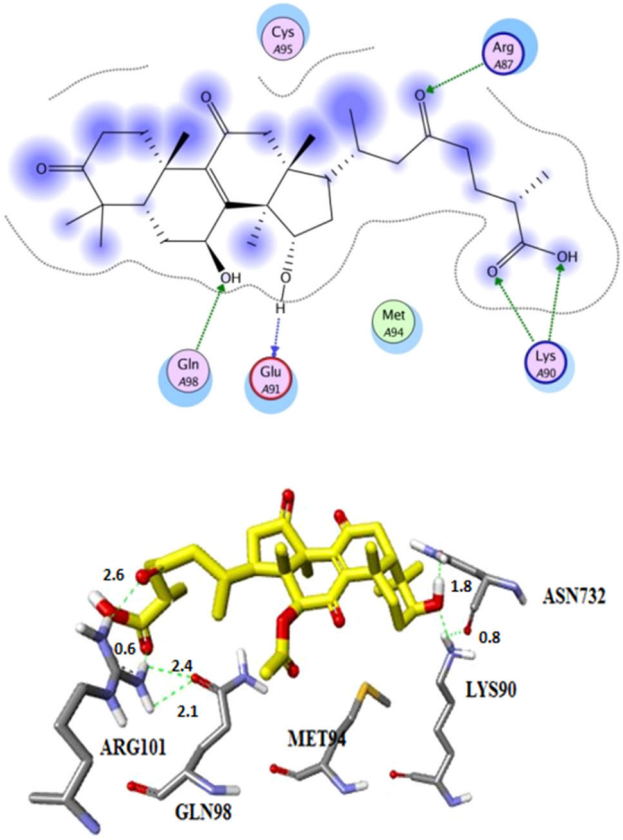

Fig. 7 In GA-F, an electrostatic interaction was found in Glu86 forming interhydrogen bonding, whereas, hydrogen bonding in Glu729:Asp725. Covalent bonding was prominently makes interaction in Asp725. Hydrogen bonding was found in Gln 98, Lys90, Arg87 and Glu91 in which Glu91 donates electron to the ligand

Ganoderic acid, possessing basic lanosterol structure, is critically involved in interaction in NEMO subunit of NF-κB. *In vitro*, it has been experimentally demonstrated that GA-A and GA-H effectively inhibit the breast cancer, whereas GA-F does not. Mechanistically, unrevealed till now is that bioinformatics tools enhance the prospect of design and synthesis of effective drugs devoid of detrimental effects. Molecular docking highlighted the possible sites or residues which play a role in effective inhibition of breast cancer. Significantly, interactive forces control and retain the stability of the structure. Ganoderic acids (GA-A and GA-H) interact with residues in the cavities (85–105), prominently in Lys90, Asn732, Glu91, Met94 and Glu98. Lys90 is a crucial residue interacting via hydrogen bonding with oxygen of GA-H, whereas Asp732 and Arg87 interact with NEMO (Figs. 4, 5). Various interactive factors favorable for stability viz hydrogen bonding and van der Waals forces were observed in GA-A and GA-H, but not in GA-F. In GA-F, Lys90 and Asp732 interact with oxygen but in positions different from GA-A and GA-H, thus exhibiting different activities. Other residues such as Arg101 and Glu98 were also involved in binding which might be different from the usual interaction (Fig. 6). This binding pattern different from above interaction makes them ineffective against breast cancer. In spite of this, different parameters are involved in effective binding of ligand to the NEMO, particularly binding energy, ligand efficiency, inhibition constant, intermolecular energy, Van der Waals desolvation energy, electrostatic energy, total energy, torsional energy and unbound energy. Protein-binding complex is a reliable scoring function based on top binding scores. Binding is considered successful if rmsd value $\leq$2 A° which is widely accepted. In ganoderic acid, binding energy is almost similar to that of the protein and does not show any remarkable conclusion, whereas, residues involved during active site were less common and present in little number in GA-F as compared to GA-A and GA-H.

Conclusion

NF-κB is a hot spot research area in biological, biochemical and pharmacological research for determining the regulation of protein expression at particular level. It is an ordeal to synthesize effective drugs without exploring decisive dimensions considered a vital prerequisite to any drug design and synthesis program. Molecular homology has bridged the gap between the design and the development of drugs, providing right platform for the synthesis of effectual drugs by targeting various possible sites of naturally occurring ganoderic acid. Ganoderic acids A and H were mechanistically proven to exhibit the biological activities as claimed umpteen times in the literature reports. The docking study carried out helped in understanding the role of substitution in portrayal and modification of various biological activities. Hydroxyl group at C-7 and C-15 in GA-A and at C-3 in GA-H, as seen through docking, participates in interactions that contribute toward their inhibitory potential. On the contrary, in GA-F, the presence of carbonyl groups and the absence of hydroxyl group restrict the interactions, thus not contributing toward any bioactivity. Moreover, the steroidal scaffold possessed by the ganoderic acids A and H makes them adept enough to fit snugly in the docking cavity of the nuclear transcription factor. Thus, the computational analysis carried out provided a rationalization of the ability of naturally occurring GA-A and GA-H to alter the NF-κB signaling pathway. Further studies about interactions of ganoderic acid with NF-κB would assist in the synthesis of better and efficacious pharmacophore incorporated with appropriate substituents for the rational designing of numerous anticancer drugs.

Acknowledgments Authors thank Central University of Punjab, Bathinda, for providing the necessary facilities to carry out the present work.

References

Agou F, Ye F, Goffinont S, Courtois G, Yamaoka S, Israël A, Véron M (2002) NEMO trimerizes through its coiled-coil C-terminal domain. J Biol Chem 277:17464–17475

Allgayer H (2010) Pdcd4, a colon cancer prognostic that is regulated by a microRNA. Crit Rev Oncol/Hematol 73:185–191

Biswas DK, Shi Q, Baily S, Strickland I, Ghosh S, Pardee AB, Iglehart JD (2004) NF-κB activation in human breast cancer specimens and its role in cell proliferation and apoptosis. Proc Natl Acad Sci USA 101:10137–10142

Chen N-H, Liu J-W, Zhong J-J (2010) Ganoderic acid T inhibits tumor invasion in vitro and in vivo through inhibition of MMP expression. Pharmacol Rep 62:150

Daschner PJ, Ciolino HP, Plouzek CA, Yeh GC (1999) Increased AP-1 activity in drug resistant human breast cancer MCF-7 cells. Breast Cancer Res Treat 53:229–240

Dolcet X, Llobet D, Pallares J, Matias-Guiu X (2005) NF-kB in development and progression of human cancer. Virchows Arch 446:475–482

Fasshauer D, Sutton RB, Brunger AT, Jahn R (1998) Conserved structural features of the synaptic fusion complex: SNARE proteins reclassified as Q-and R-SNAREs. Proc Natl Acad Sci 95:15781–15786

Ghosh S, Karin M (2002) Missing pieces in the NF-κB puzzle. Cell 109:S81–S96

Giuliani C, Napolitano G, Bucci I, Montani V, Monaco F (2001) Nf-kB transcription factor: role in the pathogenesis of inflammatory, autoimmune, and neoplastic diseases and therapy implications]. La Clin Terapeutica 152:249

Grover A, Shandilya A, Punetha A, Bisaria VS, Sundar D (2010) Inhibition of the NEMO/IKKβ association complex formation, a novel mechanism associated with the NF-κB activation suppression by Withania somnifera's key metabolite withaferin A. BMC Genom 11:S25

Jiang J, Grieb B, Thyagarajan A, Sliva D (2008) Ganoderic acids suppress growth and invasive behavior of breast cancer cells by modulating AP-1 and NF-κB signaling. Int J Mol Med 21: 577–584

Marienfeld RB, Palkowitsch L, Ghosh S (2006) Dimerization of the IκB kinase-binding domain of NEMO is required for tumor necrosis factor alpha-induced NF-κB activity. Mol Cell Biol 26:9209–9219

May MJ, Marienfeld RB, Ghosh S (2002) Characterization of the IκB-kinase NEMO binding domain. J Biol Chem 277:45992–46000

Rushe M, Silvian L, Bixler S, Chen LL, Cheung A, Bowes S, Cuervo H, Berkowitz S, Zheng T, Guckian K (2008) Structure of a NEMO/IKK-associating domain reveals architecture of the interaction site. Structure 16:798–808

Schomer-Miller B, Higashimoto T, Lee Y-K, Zandi E (2006) Regulation of IκB kinase (IKK) complex by IKKγ-dependent phosphorylation of the T-loop and C terminus of IKKβ. J Biol Chem 281:15268–15276

Sliva D (2004) Signaling pathways responsible for cancer cell invasion as targets for cancer therapy. Curr Cancer Drug Targets 4:327–336

Suarez-Arroyo IJ, Rosario-Acevedo R, Aguilar-Perez A, Clemente PL, Cubano LA, Serrano J, Schneider RJ, Martínez-Montemayor MM (2013) Anti-tumor effects of ganoderma lucidum (Reishi) in inflammatory breast cancer in vivo and in vitro models. PLoS ONE 8:e57431

Tak PP, Firestein GS (2001) NF-κB: a key role in inflammatory diseases. J Clin Invest 107:7–11